XI Workshop Brasileiro 2019 Micro Meteorologia
20 a 22 de novembro de 2019 | INPE | São José dos Campos - SP | Brasil

MEAN SCALAR PROFILES FROM LARGE-EDDY SIMULATION

Livia S. Freire[1]

[1]Instituto de Ciências Matemáticas e de Computação, USP

Resumo

Simulação de Grandes Vórtices (LES, sigla em inglês) é uma ferramenta importante no estudo de escoamentos geofísicos, mas a escolha do modelo subgrid e método numérico pode ter impactos relevantes nos resultados. Neste estudo, o impacto de três modelos subgrid baseados no modelo de Smagorinsky (constante, dinâmico e lagrangeano dinâmico dependente de escalas) no transporte de escalares simulados pelo LES é investigado. Duas opções de métodos numéricos para o campo de escalares também são testadas: volumes finitos e a combinação de método espectral (nas direções horizontais) e diferenças finitas (na direção vertical). Resultados de uma simulação de escoamento em canal neutro mostra que, além dos impactos já conhecidos no escoamento, os modelos subgrid também impactam o campo de escalares de modo diferente dependento no método numérico utilizado, gerando perfis logarítmicos com diferentes números de Schmidt em cada caso. Esse resultado demonstra que é necessário levar em conta esse tipo de erro quando resultados de LES são utilizados para validar novas teorias.

Palavras-chave: Simulação de Grandes Vórtices; Modelos Subgrid; Espectral-Diferenças Finitas; Volumes Finitos

Abstract

Large-Eddy Simulation (LES) is an important tool in the study of geophysical flows, but the choice of a subgrid-scale (SGS) model and numerical method can have a significant impact on the results. In this study, the impact of three different SGS models based on the Smagorinsky approach (constant, dynamic and scale-depedent lagrangian dynamic) on the passive scalar field generated by LES is investigated. Two numerical methods for the scalar field are also tested: finite volume and a combination of spectral (in the horizontal directions) with finite difference (in the vertical direction). Results from a neutral channel-flow simulation show that, in addition to the well known impact on the flow field, the SGS models also impact the scalar field in different ways depending on the numerical method used, generating log-law profiles with different turbulent Schmidt numbers on each case. This result demonstrates the need to take this type of error into account when using LES to validate new theories.

Keywords: Large-Eddy Simulation; Subgrid-Scale Models; Spectral-Finite Difference; Finite Volume

1. Introduction

Large-Eddy Simulation (LES) is an important tool in the study of the Atmospheric Boundary Layer (ABL), providing relevant information on the behavior of turbulence structures and the resulting transport of matter and energy under different meteorological and surface conditions (SHAW; SCHUMANN, 1992; WU; WANG; WANG, 2008; XIE; CASTRO, 2009; PATTON et al., 2016; BRUN; BLEIN; CHOLLET, 2017; BAO; CHOW; LUNDQUIST, 2018; WANG; LI; WANG, 2018). In LES, all variables are filtered for small-scale removal, significantly reducing the computational cost while maintaining most of the kinetic energy of the flow. The governing equations are obtained by filtering Navier-Stokes

and continuity equations, which (for incompressible flow) corresponds to

$$\frac{\partial \widetilde{u}_i}{\partial t} + \frac{\partial \widetilde{u_i u_j}}{\partial x_j} = -\frac{1}{\rho}\frac{\partial \widetilde{p}}{\partial x_i} + \nu \frac{\partial^2 \widetilde{u}_i}{\partial x_j x_j} + F_i, \tag{1}$$

$$\frac{\partial \widetilde{u}_i}{\partial x_i} = 0, \tag{2}$$

where $\widetilde{u}_i$ is the filtered velocity field, $\widetilde{p}$ is the filtered pressure field, ν is the kinematic viscosity of air and F_i is the mean streamwise pressure forcing (POPE, 2000).

In order to close this set of equations, the second term on the left-hand-side of Eqn. (1) needs to be rewritten as a function of the resolved velocity $\widetilde{u}_i$ and pressure $\widetilde{p}$. By defining the residual stress tensor

$$\tau_{ij}^R \equiv \widetilde{u_i u_j} - \widetilde{u}_i \widetilde{u}_j \tag{3}$$

and the residual kinetic energy

$$e^R \equiv \frac{1}{2}\tau_{ii}^R, \tag{4}$$

it is possible to write

$$\widetilde{u_i u_j} = \tau_{ij} + \frac{2}{3} e^R \delta_{ij} + \widetilde{u}_i \widetilde{u}_j, \tag{5}$$

where τ_{ij} is the anisotropic part of the residual stress tensor ($\tau_{ij} = \tau_{ij}^R - 2e^R\delta_{ij}/3$), also known as subgrid-scale (SGS) stress tensor. The final Navier-Stokes equation for LES can be written as (BOU-ZEID; MENEVEAU; PARLANGE, 2005)

$$\frac{\partial \widetilde{u}_i}{\partial t} + \frac{\partial \widetilde{u}_i \widetilde{u}_j}{\partial x_j} = -\frac{1}{\rho}\frac{\partial \widetilde{p}*}{\partial x_i} + \frac{\partial \tau_{ij}}{\partial x_j} + F_i, \tag{6}$$

where $\widetilde{p}^* = \widetilde{p} + \frac{2}{3}\rho e^R$ is a modified pressure. Note that because molecular viscosity can be neglected in the resolved scales of atmospheric flow, it was removed from Eqn. (6). The impact of the unsolved part of the flow on the resolved velocity field is represented by τ_{ij}, which is the term that needs to be parameterized as a function of the resolved velocity field.

A diverse set of parameterizations, known as SGS models, has been developed for different applications and numerical approaches. Based on the eddy-viscosity and mixing-length assumptions, the first and more traditional model was developed by Smagorinsky (1963), corresponding to

$$\tau_{ij} = -2\nu_{SGS}\widetilde{S}_{ij} = -2(C_s\Delta)^2|\widetilde{S}|\widetilde{S}_{ij}, \tag{7}$$

where ν_{SGS} is the SGS eddy viscosity, $\widetilde{S}_{ij} = \frac{1}{2}\left(\frac{\partial \widetilde{u}_i}{\partial x_j} + \frac{\partial \widetilde{u}_j}{\partial x_i}\right)$ is the resolved strain rate tensor ($|\widetilde{S}|$ is its magnitude), Δ is the filter size and C_s is the Smagorinsky coefficient, a new unknown in the set of equations. The value of C_s can be assumed as constant (LILLY, 1967) or can be estimated based on the information resolved by the simulation (GERMANO et al., 1991; BOU-ZEID; MENEVEAU; PARLANGE, 2005). The choice of C_s modeling can impact the resolved field in different ways depending on the type of flow, and it can be evaluated by comparing the statistics of the velocity field with well-established theoretical, experimental or numerical results. As any parameterization, no perfect solution exists, and the search for SGS models more suitable for different applications is an ongoing research field.

Another source of errors in LES is the numerical methods adopted for solving the flow and scalar fields. Every type of numerical discretization has its own advantages and downsides, which also can be assessed by confronting the results with the known theories of the simulated flow. For example, spectral methods provide high accuracy and variance conserving properties, making it the primary choice for flow simulation in homogeneous directions, but it can also generate unphysical negative concentrations when used to simulate scalar concentration fields (CHAMECKI; MENEVEAU; PARLANGE, 2008). Due to these potential errors, previous studies have investigated the impact of different numerical and SGS approaches on the flow field (KHANNA; BRASSEUR, 1997; BOU-ZEID; MENEVEAU; PARLANGE, 2005; BRASSEUR; WEI, 2010), but their impact on passive scalar

transport has not been explored. Given the use of LES to test new equations for scalar statistics in the ABL (CHAMECKI; MENEVEAU, 2011; FREIRE; CHAMECKI; GILLIES, 2016; GERKEN; CHAMECKI; FUENTES, 2017; NISSANKA et al., 2018), it is important to know which potential impacts SGS and numerical methods may have on the scalar field produced by LES.

In this study, the impact of three different SGS models and two numerical approaches on the simulation of scalar transport in LES is investigated. A LES code developed for ABL simulations is used to simulate a channel flow with passive scalar. The choice of channel flow is justified by the existence of a theoretical mean scalar concentration profile, which will be used to test the LES results, and by the overall similarity with ABL flows.

2. LES code and simulation setup

The LES code used in the present study was developed for ABL simulations under different stability conditions (BOU-ZEID; MENEVEAU; PARLANGE, 2005; KLEISSL et al., 2006). The simulation of the flow field is performed by a pseudo-spectral code in horizontal directions, a second-order centered-finite difference code in the vertical direction and a fully explicit second-order Adams-Bashforth scheme for time advancement. Boundary conditions are periodic in horizontal directions, stress-free at the top of the domain and a law-of-the-wall formulation at the bottom. Three different SGS models are tested, namely (1) a constant C_s with a wall damping function as proposed by Mason e Thomson (1992), (2) the dynamic model proposed by Germano et al. (1991) and (3) the scale-dependent lagrangian dynamic model proposed by Bou-Zeid, Meneveau e Parlange (2005). While the impact of these three SGS models on the flow field was tested by Bou-Zeid, Meneveau e Parlange (2005), their impact on scalar transport has not yet been evaluated.

In addition to the three SGS models, two numerical methods for scalar field are also tested: the first one corresponds to the same numerical method adopted for the flow field (spectral plus finite difference, SFD) and the second method corresponds to the approach developed by Chamecki, Meneveau e Parlange (2008), which uses a divergence-free interpolated velocity field from the original SFD method to transport the scalar simulated by the finite volume method (FV). Both codes are simulated simultaneously, i.e., the scalar is transported by the same instantaneous velocity field.

Three simulations were performed separatelly, one for each SGS model. The SGS eddy diffusivity (needed for the SGS scalar flux) is defined as $D_{SGS} = \nu_{SGS}/Sc$, where $Sc = 0.4$ is a constant SGS turbulent Schmidt number adopted here for both scalar numerical methods. Simulation parameters are equal to the ones performed by Bou-Zeid, Meneveau e Parlange (2005), namely: a domain of $L \times L \times H = 2\pi \times 2\pi \times 1\,\mathrm{m}^3$ with 64^3 grid points, a roughness length z_0 of $1 \times 10^{-4}\,\mathrm{m}$, an imposed mean pressure gradient force $F_i = (1,0,0)\,\mathrm{m\,s^{-2}}$, time steps of $2.5 \times 10^{-4}\,\mathrm{s}$ and a total of $200\,000$ time steps. Both scalar fields (SFD from the spectral-finite difference code and FV from the finite volume code) were initialized with zero concentration, and a constant surface flux equal to $0.2\,\mu\mathrm{g\,m^{-2}s^{-1}}$ were applied. Results presented next correspond to averages in both horizontal directions and during the last $20\,000$ time steps.

3. Results and Discussion

From boundary-layer theory, we know that a turbulent channel flow without buoyancy (i.e., neutral flow) has a region with mean streamwise velocity proportional to the logarithm of the distance from the wall (known as law-of-the-wall), in which the following equations are valid:

$$\frac{\overline{u}}{u_*} = \frac{1}{\kappa} \ln\left(\frac{z}{z_0}\right), \tag{8}$$

$$\frac{\kappa z}{u_*}\frac{d\overline{u}}{dz} = \phi_m = 1, \tag{9}$$

$$\frac{\overline{c}}{\overline{c}_r} = 1 - \frac{Sc_t \Phi}{\kappa u_* \overline{c}_r} \ln\left(\frac{z}{z_r}\right), \tag{10}$$

$$\frac{\kappa z}{c_*}\frac{d\overline{c}}{dz} = \phi_c = Sc_t, \tag{11}$$

where $\overline{u}$ is the mean streamwise velocity, u_* is the friction velocity, z is height, z_0 is the roughness length, κ is the Von Kármán constant, ϕ_m and ϕ_c are the nondimensional velocity and scalar gradients,

respectively, $\overline{c}$ is the mean scalar concentration, $\overline{c}_r$ is the mean concentration at a reference height z_r, $\Phi = \overline{w'c'}_0$ is the net scalar surface flux, $c_* = -\Phi/u_*$ is the scalar scale, and Sc_t is the turbulent Schmidt number. The exact value of Sc_t (or turbulent Prandtl number Pt_t when the scalar corresponds to a passive heat) or even its existence is still an open question, but laboratory experiments indicate values in the range between 0.73 and 0.92 (KAYS, 1994; LI, 2019). When using LES to validate new theories, it is important to note that any deviation from Eqns. (8)–(11), in addition to the value of Sc_t from the LES, needs to be taken into account as potential source of errors. The region of the flow where the law-of-the-wall is expected to hold corresponds to lower 10% of the vertical domain, approximately (as the viscous sublayer is not captured by this LES).

To validate the simulations, Figure 1 reproduces the results presented by Bou-Zeid, Meneveau e Parlange (2005), which shows the impact of different SGS models on the flow. The constant model, which applies the profile presented in Figure 1 (first plot) in the entire horizontal domain, generates a mean velocity profile close to Eqn. (8), but the value of ϕ_m presents an significant overestimation in the lower grid points. Note also that for the constant model the SGS shear stress is higher than the other models close to the wall, and the variances are lower. These features are in agreement with the knowledge that the constant model is overdissipative (PORTé-AGEL; MENEVEAU; PARLANGE, 2000). The dynamic model, which calculates a layer-by-layer C_s based on the resolved stress tensor (it compares the SGS model applied in a resolved scale with the corresponding resolved stress, averaging over horizontal planes and evolving with the simulation), presents the opposite behavior of the constant model, i.e., it is underdissipative. The scale-dependent lagrangian dynamic model, which not only averages the value of C_s in time following fluid pathlines (therefore it can be applied in non-homogeneous simulations) but it also takes into account scale effects in the dynamic model, generates the results closest to the law-of-the-wall. For this reason, the latter has become the most used SGS model for this LES code in studies of atmospheric and oceanic boundary layer (CHEN et al., 2016; FREIRE; CHAMECKI; GILLIES, 2016; GIOMETTO et al., 2016; GERKEN; CHAMECKI; FUENTES, 2017; RAMUDU et al., 2018; STEVENS; MARTíNEZ-TOSSAS; MENEVEAU, 2018). For a detailed discussion on the comparison between these SGS models, see Bou-Zeid, Meneveau e Parlange (2005).

Figure 2 presents scalar profiles for each SGS model and for both numerical methods tested. For the constant SGS model, results of scalar concentration, gradient and turbulent flux are similar between SFD and FV, with profiles and gradients matching Eqn. (10) and (11) with a value of Sc_t transitioning from about 0.55 to 1.1. The use of the dynamic model or the scale-dependent lagrangian model generates different scalar fields: while FV results correspond to $Sc_t \approx 1$, SFD results are closer to $Sc_t = 0.6$. This difference reinforces the need to take the numerical method into account when evaluating LES results.

When looking at the results close to the wall, by using the dynamic model (or the scale-dependent lagrangian dynamic model) the resolved part of the turbulent flux is larger than the constant model. This indicates that the cause for different results between FV and SFD might be in the resolved flow close to the wall (a cause that is being “erased” in the constant model by the overdissipation of energy). Therefore, one possible approach to try to match the scalar fields from FV and SFD is to apply a SGS model made specifically for each case, in order to compensate the differences created in the resolved field. This option will be explored in future studies.

4. Conclusion

LES is an important tool in the study of the ABL, but the errors of the SGS model and the numerical method adopted need to be taken into account. SGS models that have been developed for improvements in the flow field are not necessarily optimized for scalar transport, especially if a different numerical method is used. Therefore, when using LES results to validate new theories and models, it is important to be aware of the uncertainty caused by the errors from the LES.

Channel flow is a good starting point in the evaluation of LES results because, in addition to the similarity with ABL flows, it has theoretical results that has been validated by different laboratory and numerical experiments. For this type of simulation it was observed that a scalar field generated by a finite volume code is different from the one generated by the scalar-finite difference method. It is possible that this difference is a result of the interpolation needed to adapt the SFD velocity field

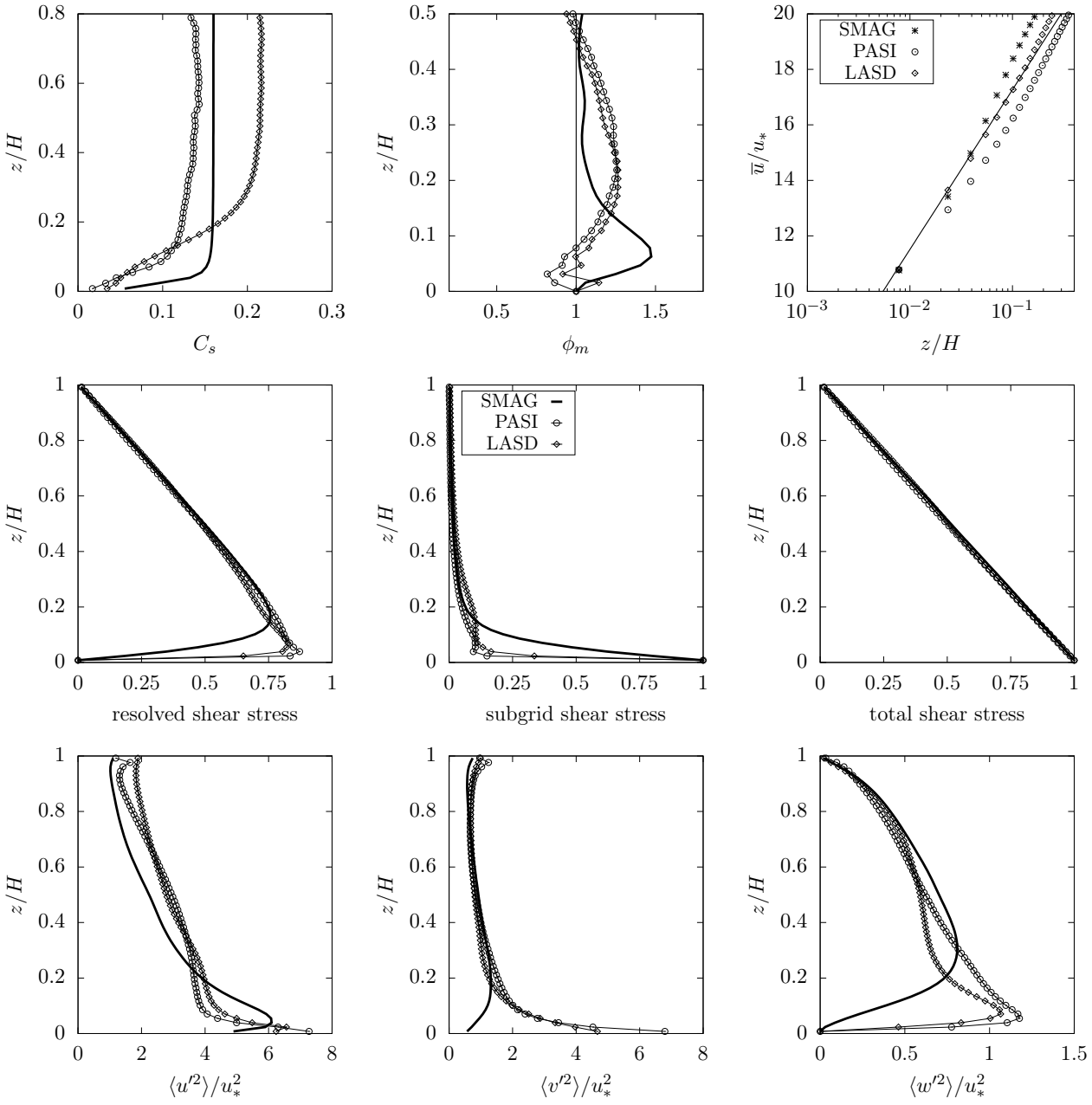

Figura 1 – Vertical profiles of flow statistics from constant model (SMAG), dynamic model (PASI) and scale-dependent lagrangian dynamic model (LASD). Upper panels: Smagorinsky coefficient (left), nondimensional vertical gradient of streamwise velocity (center), mean streamwise velocity (right). Middle panels: resolved (left), subgrid (center) and total (right) shear stress. Bottom panels: variance of streamwise (left), spanwise (middle) and vertical (right) velocity. Solid thin lines correspond to Eqns. (8) and (9).

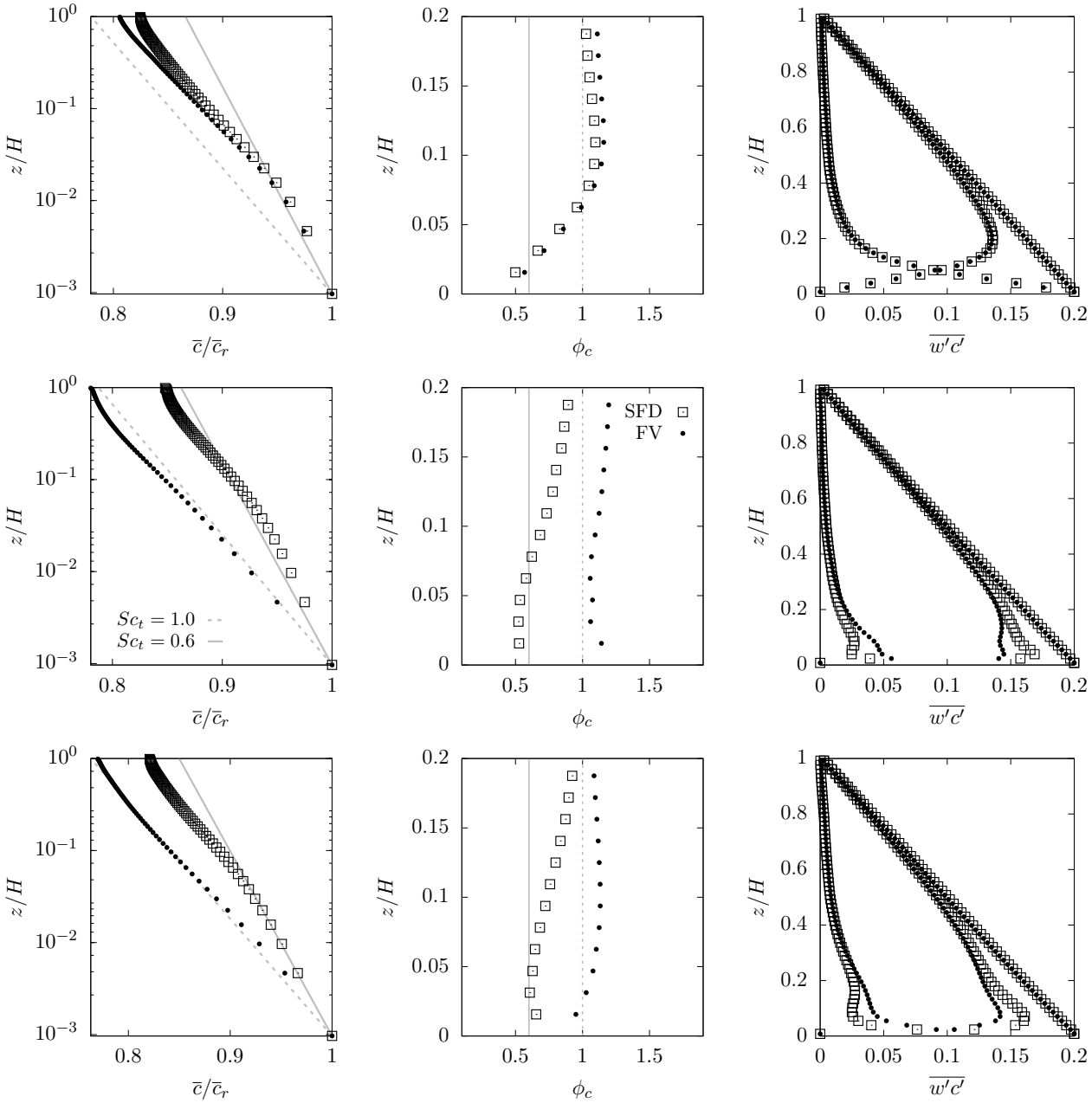

Figura 2 – Vertical profiles of scalar statistics: mean concentration (left), normalized vertical gradient of concentration (center), subgrid, resolved and total scalar fluxes (right). Upper panels correspond to constant model, middle panels correspond to dynamic model, and bottom panels correspond to scale-dependent lagrangian dynamic model.

to the FV model. Future work should evaluate this interpolated velocity field in more details, and investigate if this behavior is consistent across different types of ABL simulations (different thermal stabilities, u_*, ABL height, and so on).

Acknowledgements

This study was funded by São Paulo Research Foundation (FAPESP, grants 2018/24284-1 and 2019/14371-7) and supported by the Mathematical Science Center Applied to Industry (CEPID-CeMEAI) through the use of the Cluster Euler.

Referências Bibliográficas

BAO, J.; CHOW, F. K.; LUNDQUIST, K. A. Large-eddy simulation over complex terrain using an improved immersed boundary method in the weather research and forecasting model. **Monthly Weather Review**, v. 146, n. 9, p. 2781–2797, 2018. Disponível em: <https://doi.org/10.1175/MWR-D-18-0067.1>.

BOU-ZEID, E.; MENEVEAU, C.; PARLANGE, M. A scale-dependent lagrangian dynamic model for large eddy simulation of complex turbulent flows. **Physics of Fluids**, AIP, v. 17, n. 2, p. 025105, 2005. Disponível em: <http://dx.doi.org/10.1063/1.1839152>.

BRASSEUR, J. G.; WEI, T. Designing large-eddy simulation of the turbulent boundary layer to capture law-of-the-wall scaling. **Physics of Fluids**, v. 22, n. 2, p. 021303, 2010. Disponível em: <http://scitation.aip.org/content/aip/journal/pof2/22/2/10.1063/1.3319073>.

BRUN, C.; BLEIN, S.; CHOLLET, J.-P. Large-eddy simulation of a katabatic jet along a convexly curved slope. part i: Statistical results. **Journal of the Atmospheric Sciences**, v. 74, n. 12, p. 4047–4073, 2017. Disponível em: <https://doi.org/10.1175/JAS-D-16-0152.1>.

CHAMECKI, M.; MENEVEAU, C. Particle boundary layer above and downstream of an area source: scaling, simulations, and pollen transport. **Journal of Fluid Mechanics**, v. 683, p. 1–26, 2011. ISSN 1469-7645. Disponível em: <http://dx.doi.org/10.1017/jfm.2011.243>.

CHAMECKI, M.; MENEVEAU, C.; PARLANGE, M. A hybrid spectral/finite-volume algorithm for large-eddy simulation of scalars in the atmospheric boundary layer. **Boundary-Layer Meteorology**, Springer Netherlands, v. 128, n. 3, p. 473–484, 2008. ISSN 0006-8314. Disponível em: <http://dx.doi.org/10.1007/s10546-008-9302-1>.

CHEN, B.; YANG, D.; MENEVEAU, C.; CHAMECKI, M. Effects of swell on transport and dispersion of oil plumes within the ocean mixed layer. **Journal of Geophysical Research: Oceans**, v. 121, n. 5, p. 3564–3578, 2016. Disponível em: <https://agupubs.onlinelibrary.wiley.com/doi/abs/10.1002/2015JC011380>.

FREIRE, L. S.; CHAMECKI, M.; GILLIES, J. A. Flux-profile relationship for dust concentration in the stratified atmospheric surface layer. **Boundary-Layer Meteorology**, v. 160, n. 2, p. 249–267, 2016. ISSN 1573-1472. Disponível em: <http://dx.doi.org/10.1007/s10546-016-0140-2>.

GERKEN, T.; CHAMECKI, M.; FUENTES, J. D. Air-parcel residence times within forest canopies. **Boundary-Layer Meteorology**, v. 165, n. 1, p. 29–54, Oct 2017. ISSN 1573-1472. Disponível em: <https://doi.org/10.1007/s10546-017-0269-7>.

GERMANO, M.; PIOMELLI, U.; MOIN, P.; CABOT, W. H. A dynamic subgrid-scale eddy viscosity model. **Physics of Fluids A**, v. 3, n. 7, p. 1760–1765, 1991. Disponível em: <http://dx.doi.org/10.1063/1.857955>.

GIOMETTO, M. G.; CHRISTEN, A.; MENEVEAU, C.; FANG, J.; KRAFCZYK, M.; PARLANGE, M. B. Spatial characteristics of roughness sublayer mean flow and turbulence over a realistic urban surface. **Boundary-Layer Meteorology**, v. 160, n. 3, p. 425–452, Sep 2016. ISSN 1573-1472. Disponível em: <https://doi.org/10.1007/s10546-016-0157-6>.

KAYS, W. M. Turbulent prandtl number – where are we? **Journal of Heat Transfer**, The American Society of Mechanical Engineers, v. 116, p. 284–295, 1994. Disponível em: <http://gen.lib.rus.ec/scimag/index.php?s=10.1115/1.2911398>.

KHANNA, S.; BRASSEUR, J. G. Analysis of monin–obukhov similarity from large-eddy simulation. **Journal of Fluid Mechanics**, Cambridge University Press, v. 345, p. 251–286, 1997. Disponível em: <http://dx.doi.org/10.1017/S0022112097006277>.

KLEISSL, J.; KUMAR, V.; MENEVEAU, C.; PARLANGE, M. B. Numerical study of dynamic smagorinsky models in large-eddy simulation of the atmospheric boundary layer: Validation in stable and unstable conditions. **Water Resources Research**, v. 42, n. 6, p. W06D09, 2006. ISSN 1944-7973. Disponível em: <http://dx.doi.org/10.1029/2005WR004685>.

LI, D. Turbulent prandtl number in the atmospheric boundary layer - where are we now? **Atmospheric Research**, v. 216, p. 86 – 105, 2019. ISSN 0169-8095. Disponível em: <http://www.sciencedirect.com/science/article/pii/S0169809518307324>.

LILLY, D. K. The representation of small-scale turbulence in numerical simulation experiments. In: **Proc. IBM Scientific Computing Symposium on Environmental Sciences**. [S.l.: s.n.], 1967. p. 195.

MASON, P. J.; THOMSON, D. J. Stochastic backscatter in large-eddy simulations of boundary layers. **Journal of Fluid Mechanics**, v. 242, p. 51–78, 9 1992. ISSN 1469-7645. Disponível em: <http://dx.doi.org/10.1017/S0022112092002271>.

NISSANKA, I. D.; PARK, H. J.; FREIRE, L. S.; CHAMECKI, M.; REID, J. S.; RICHTER, D. H. Parameterized vertical concentration profiles for aerosols in the marine atmospheric boundary layer. **Journal of Geophysical Research: Atmospheres**, v. 123, p. 9688—-9702, 2018. Disponível em: <http://dx.doi.org/10.1029/2018JD028820>.

PATTON, E. G.; SULLIVAN, P. P.; SHAW, R. H.; FINNIGAN, J. J.; WEIL, J. C. Atmospheric stability influences on coupled boundary layer and canopy turbulence. **Journal of the Atmospheric Sciences**, v. 73, n. 4, p. 1621–1647, 2016. Disponível em: <http://dx.doi.org/10.1175/JAS-D-15-0068.1>.

POPE, S. B. **Turbulent Flows**. [S.l.]: Cambridge University Press, 2000.

PORTé-AGEL, F.; MENEVEAU, C.; PARLANGE, M. B. A scale-dependent dynamic model for large-eddy simulation: application to a neutral atmospheric boundary layer. **Journal of Fluid Mechanics**, v. 415, p. 261–284, 7 2000. ISSN 1469-7645. Disponível em: <http://dx.doi.org/10.1017/S0022112000008776>.

RAMUDU, E.; GELDERLOOS, R.; YANG, D.; MENEVEAU, C.; GNANADESIKAN, A. Large eddy simulation of heat entrainment under arctic sea ice. **Journal of Geophysical Research: Oceans**, v. 123, n. 1, p. 287–304, 2018. Disponível em: <https://agupubs.onlinelibrary.wiley.com/doi/abs/10.1002/2017JC013267>.

SHAW, R. H.; SCHUMANN, U. Large-eddy simulation of turbulent flow above and within a forest. **Boundary-Layer Meteorology**, v. 61, n. 1, p. 47–64, 1992. ISSN 1573-1472. Disponível em: <http://dx.doi.org/10.1007/BF02033994>.

SMAGORINSKY, J. General circulation experiments with the primitive equations i. the basic experiment. **Monthly Weather Review**, v. 91, n. 3, p. 99–164, march 1963. Disponível em: <http://dx.doi.org/10.1175/1520-0493(1963)091<0099:GCEWTP>2.3.COand2>.

STEVENS, R. J.; MARTíNEZ-TOSSAS, L. A.; MENEVEAU, C. Comparison of wind farm large eddy simulations using actuator disk and actuator line models with wind tunnel experiments. **Renewable Energy**, v. 116, p. 470 – 478, 2018. ISSN 0960-1481. Disponível em: <http://www.sciencedirect.com/science/article/pii/S0960148117308339>.

WANG, C.; LI, Q.; WANG, Z.-H. Quantifying the impact of urban trees on passive pollutant dispersion using a coupled large-eddy simulation–lagrangian stochastic model. **Building and Environment**, v. 145, p. 33 – 49, 2018. ISSN 0360-1323. Disponível em: <http://www.sciencedirect.com/science/article/pii/S0360132318305626>.

WU, C.; WANG, M.; WANG, L. Large-eddy simulation of formation of three-dimensional aeolian sand ripples in a turbulent field. **Science in China Series G: Physics, Mechanics and Astronomy**, SP Science in China Press, v. 51, n. 8, p. 945–960, 2008. ISSN 1672-1799. Disponível em: <http://dx.doi.org/10.1007/s11433-008-0118-2>.

XIE, Z.-T.; CASTRO, I. P. Large-eddy simulation for flow and dispersion in urban streets. **Atmospheric Environment**, v. 43, n. 13, p. 2174 – 2185, 2009. ISSN 1352-2310. Disponível em: <http://www.sciencedirect.com/science/article/pii/S135223100900034X>.